fractal and fractional

MDPI

Article

Adaptive Neural Network Synchronization Control for Uncertain Fractional-Order Time-Delay Chaotic Systems

Wenhao Yan, Zijing Jiang, Xin Huang and Qun Ding *

Electronic Engineering College, Heilongjiang University, Harbin 150080, China
* Correspondence: 1984008@hlju.edu.cn

Abstract: We propose an adaptive radial basis (RBF) neural network controller based on Lyapunov stability theory for uncertain fractional-order time-delay chaotic systems (FOTDCSs) with different time delays. The controller does not depend on the system model and can achieve synchronous control under the condition that nonlinear uncertainties and external disturbances are completely unknown. Stability analysis showed that the error system asymptotically tended to zero in combination with the relevant lemma. Numerical simulation results show the effectiveness of the controller.

Keywords: radial basis neural network; Lyapunov stability theory; fractional-order time-delay chaotic system

check for updates

Citation: Yan, W.; Jiang, Z.; Huang, X.; Ding, Q. Adaptive Neural Network Synchronization Control for Uncertain Fractional-Order Time-Delay Chaotic Systems. *Fractal Fract.* **2023**, *7*, 288. https://doi.org/10.3390/fractalfract7040288

Academic Editor: Gani Stamov

Received: 28 January 2023
Revised: 1 March 2023
Accepted: 17 March 2023
Published: 27 March 2023

1. Introduction

The theory of fractional calculus has been developed for more than 300 years, but due to a lack of effective computing means, its research has been in the field of pure mathematics, and its development has been slow. With the continuous development of computer technology, the application of fractional calculus in engineering practice and physics has become a hotspot [1–4]. Compared with integer-order differential equations, fractional-order calculus equations can describe natural phenomena more accurately [5,6]. Therefore, they are universal to studying fractional-order systems.

Chaos is a special movement state of a nonlinear system that is the unity of order and disorder; it is easily affected by external conditions and especially sensitive to the initial value of the system. With the gradual deepening of people's understanding of chaotic systems, scholars have found that fractional-order chaotic systems have almost all the characteristics of integer-order chaotic systems. Because of their historical memory characteristics, fractional-order chaotic systems often have more complex dynamic behaviors than those of integer-order chaotic systems. Time delay is a common phenomenon in nature [7]. Due to the influence of friction, machinery, and other practical factors, there are always time delays in practical systems, such as physics, machinery, economy, biology, and engineering. In addition, time delay has an important impact on the dynamic characteristics of the system. When the change in the system on both the current and past states, the system is called a time-delay system. The existence of a time delay renders the fractional chaotic system more complex, and has broad application prospects in image encryption [8], secure communication [9], and biomedicine [10].

Chaos synchronization control means that the state trajectory of the response system can completely follow the drive system under the action of the controller. In 1990, chaos synchronization was first proposed by Pecora and Carroll, who successfully realized the synchronization of two systems with the same structure under different initial conditions [11]. As a typical feature of nonlinear systems, the synchronization of chaotic systems has been studied extensively, and a large number of synchronization control methods were proposed [12–17]. In [18], a linear controller was designed for the synchronization control of fractional-order financial chaotic systems with time delay in the absence of uncertainties and external disturbances. This controller realized the active synchronization control of

fractional-order Financial chaotic systems with time delay. Liu et al. [19] investigated a sliding-mode controller that had been designed for the synchronization control of FOTDCSs with uncertainties. The controller realized the self-synchronization of FOTDCSs, but required that uncertainties be bounded and did not consider external disturbances. In addition, the controller could not achieve synchronization with different structures. In [20,21], the authors adopted active control to directly eliminate the nonlinear term, rendering the coefficient matrix of the system constant and realizing the hybrid projection synchronization of FOTDCSs. However, its control cost was large, and when there were unknown uncertainties in the system, this method could not achieve the expected control effect. Li et al. [22] realized the impulse synchronization of FOTDCSs, but the controller needed to know the coefficient matrix of the linear part of the drive and the response system, which was highly dependent on the system model. When there are uncertainties or external disturbances in the system, it is difficult for this method to achieve synchronization control. Velmurugan et al. [23] proposed hybrid projection synchronization on the basis of the neural network fractional time-delay memristor model, which also uses active control to eliminate nonlinear terms. Second, it did not consider the aging and decay of memristor elements (that is, there were unknown uncertainties in the system). Luo et al. [24] investigated the fractional-order MEMS model and achieved the active synchronization of the model through a Chebyshev neural network. However, this idea was only aimed at special models and is not universal. In addition, all the above control methods are only applicable to synchronous control when the time delays of the drive and response systems are the same.

In an actual physical system, the system may be affected by external disturbances, and the aging and attenuation of components exist in the running process of the system. The above factors hinder the ideal model from accurately describing the actual physical system. On the basis of the above considerations, this paper mainly focuses on the synchronization control of uncertain FOTDCSs based on adaptive RBF neural networks. On the one hand, an RBF neural network, as a local approximation network, could approximate any continuous function with arbitrary precision. So, an RBF neural network can be used to estimate an unknown system type. On the other hand, adaptive control can eliminate the influence of uncertainty and complex factors by automatically adjusting the relevant parameters of the controller, so that the controller could adapt to the controlled object and the environment. Under the action of the designed synchronous controller, the synchronization error asymptotically approaches zero. The novelty and contributions of this paper are as follows:

(1) On the basis of Barbarat's lemma, an adaptive RBF neural network controller was designed that realizes the synchronization control of FOTDCSs with nonlinear uncertainty and external disturbance.
(2) When the driving system and the response system have different time delays, they could also achieve synchronization under the action of the controller.
(3) A numerical simulation realized the synchronous control of the uncertain fractional time-delay Liu chaotic system and the uncertain fractional time-delay financial chaotic system. The theoretical proof and simulation results show the effectiveness of the controller.

The rest of this paper is arranged as follows: In Section 2, the preliminaries and radial basis neural network models are given. In Section 3, the synchronization controller and stability analysis based on a radial basis function neural network are presented. In Section 4, a numerical simulation is provided. Lastly, some conclusions are drawn in Section 5.

2. Preliminaries

2.1. Introduction to Fractional Calculus

There are three different definitions of fractional calculus: the Caputo derivative [25], Riemann–Liouville (R–L) derivative [26], and Grünwald–Letnikov (G–L) derivative [27]. This paper is based on Caputo's definition; the Caputo derivative is defined as follows:

$$D_t^{\alpha} f(t) = \frac{1}{\Gamma(n-\alpha)} \int_0^t \frac{f^{(n)}(\tau)}{(t-\tau)^{(\alpha-n+1)}} d\tau, \tag{1}$$

The fractional Caputo integral is defined as follows:

$$D_t^{-\alpha} f(t) = \frac{1}{\Gamma(\alpha)} \int_0^t (t-\alpha)^{(\alpha-1)} f(\tau) d\tau, \tag{2}$$

where fractional order $\alpha > 0$, and n is a smaller integer that is greater than α, namely, $n-1 < \alpha < n$. $\Gamma(\cdot)$ is the Gamma function, defined as $\Gamma(\alpha) = \int_0^t t^{(\alpha-1)} e^{-t} dt$. In addition, the fractional Caputo differential is Laplace-transformed as follows:

$$\mathscr{L}\{D_t^{\alpha} f(t), s\} = s^{\alpha} F(s) - \sum_{k=0}^{n-1} s^{\alpha-k-1} f^{(k)}(0), \tag{3}$$

where $F(s)$ is the Laplace transform of $f(t)$, and $h^{(k)}(0)$ are the initial conditions. Since the subsequent stability proof of the system needs to use the properties of fractional calculus, several properties are given in the following.

Proposition 1 ([28]). *If $x(t) \in C^1[0,T] (T > 0)$, then $D_t^{\alpha} D_t^{\alpha-1} x(t) = x(t)$.*

Proposition 2 ([29]). *If $x(t) \in R$, then there is $D_t^{\alpha-1}|x(t)| \geq 0$ and $D_t^{\alpha-1}|x(t)| \geq D_t^{\alpha-1} x(t)$.*

Proposition 3 ([30] (Barbalat's lemma)). *Set $\lim_{t\to+\infty} x^2(\tau) d\tau < \infty$, then $x(t) \in L_2$; when $x(t) \in L_\infty$, if $\dot{x}(t)$ exists and is bounded, then $\lim_{t\to+\infty} x(t) = 0$.*

Proof. Set $x(t) = D_t^{\alpha-1} e(t)$. According to Property 1, the following equation can be obtained.

$$e(t) = D_t^{\alpha-1} x(t) \tag{4}$$

By taking the Laplace transform of both sides of Equation (4), we could obtain

$$E(s) = s^{1-\alpha} X(s) - s^{-\alpha} x(0). \tag{5}$$

Via the final value theorem, we have

$$\lim_{t\to+\infty} e(t) = \lim_{s\to+0} s^{1-\alpha}(sX(s)) - \lim_{s\to 0} s^{1-\alpha}(x(0)), \tag{6}$$

$$\lim_{t\to+\infty} x(t) = \lim_{s\to+\infty} sX(s) = 0, \tag{7}$$

When $s \to 0$, $sX(s)$ and $s^{1-\alpha}$ are infinitely small, then $\lim_{s\to+0} s^{1-\alpha}(sX(s)) = 0$ and $\lim_{s\to 0} s^{1-\alpha}(x(0)) = 0$. Therefore, $\lim_{t\to+\infty} e(t) = 0$. The proof of Proposition 1 is completed. □

2.2. Introduction to Radial Basis Neural Network

The RBF neural network is widely used in pattern recognition, nonlinear control, and graph processing [31,32]. The RBF neural network is a kind of two-layer local convergence neural network, so it has fast convergence. RBF neural networks can approximate any

continuous function with arbitrary precision. The first layer is the nonlinear input layer, namely, the Gaussian basis function whose output is

$$h_j(X) = exp(\frac{-\|X - c_j\|}{2b_2^2}), (j = 1, 2, \cdots, m) \tag{8}$$

The second layer is the linear output layer whose expression is

$$y_j = \sum_{j=1}^{m} w_{ij} h_j = W_i^T H, (i = 1, 2, \cdots, n) \tag{9}$$

where $X = [X_1, X_2, \cdots, X_n]^T$ is the input vector of the RBF neural network, and the central values of $n \times m$ form the matrix $C = [c_1, c_2, \cdots, c_j, \cdots, c_m]$. $c_j = [c_{1j}, c_{2j}, \cdots, c_{ij}, \cdots, c_{nj}]^T$ and b_j are the central vector and width of the hidden layer node of the RBF neural network, respectively. $W_i = [w_{i1}, w_{i2}, \cdots, w_{im}]^T$ is the weight vector of the network, and $H = [h_1, h_2, \cdots, h_m]^T$ is the Gaussian basis function vector.

3. Design and Stability Analysis of the Adaptive Controller Based on the RBF Neural Network

3.1. Synchronization of Uncertain FOTDCSs

In this paper, an n-dimensional fractional time-delay chaotic system with uncertain terms was considered. The driving system and response system are expressed as follows:

$$D_t^\alpha x = f(x, x(t - \tau_1)) + \Delta f_1(x) + d_1(t), \tag{10}$$

$$D_t^\alpha y = g(y, y(t - \tau_2)) + \Delta f_2(x) + d_2(t) + U(t), \tag{11}$$

where $x = [x_1(t), x_2(t), \cdots, x_n(t)]^T \in R^n$, $y = [y_1(t), y_2(t), \cdots, y_n(t)]^T \in R^n$ are the measurable state variables of the driving system and the response system, respectively, and τ_1 and τ_2 are different time delays. $\Delta f(x)$ is the nonlinear uncertainty term, and $d(t)$ the external interference term. $U(t)$ is the controller to be configured.

The synchronization error is defined as $e(t) = y(t) - x(t)$. If $\lim_{t \to +0} \|e(t)\| = 0$. Then, the driving system and the response system are synchronized.

3.2. Adaptive Controller Based on the RBF Neural Network

The synchronization error system is expressed as follows:

$$\begin{aligned} D_t^\alpha e = {} & g(y, y(t - \tau_2)) - f(x, x(t - \tau_1)) + \Delta f_2(x) - \\ & \Delta f_1(x) + d_2(t) - d_1(t) + U(t). \end{aligned} \tag{12}$$

Set $\phi = g(y, y(t - \tau_2)) - f(x, x(t - \tau_1)) + \Delta f_2(x) - f_1(x) + d_2(t) - d_1(t)$, and ϕ is an unknown function. Equation (12) can be derived as follows:

$$D_t^\alpha e = \phi + U(t). \tag{13}$$

The synchronization error vector is

$$D_t^\alpha e_i = \phi_i + u_i(t). \tag{14}$$

Nonlinear function ϕ_i can be approximated with the RBF neural network:

$$\hat{\phi}_i = W_i^T H, (i = 1, 2, \cdots, n) \tag{15}$$

where H is the Gaussian basis function vector, and W_i is the weight vector of the network. The optimal estimation parameter of the RBF neural network was set to W_i^*. Then, the optimal estimation is

$$\hat{\phi}_i^* = W_i^{*T} H, \qquad (i = 1, 2, \cdots, n) \tag{16}$$

The parameter error and the optimal estimation error of the RBF neural network were set to, respectively,

$$\widetilde{W}_i = W_i - W_i^*, \qquad \rho = \phi_i - \phi_i^* \tag{17}$$

where the RBF neural network estimation error is bounded, that is, $|\rho_i| \leq \rho_i^*$, $\rho_i^* > 0$ is the upper bound of the optimal estimation error. Therefore, the estimation error of the unknown nonlinear function is

$$\phi_i - \hat{\phi}_i = \rho_i - \widetilde{W}_i^T H. \tag{18}$$

In view of the above discussion, the proposed controller is as follows:

$$U(t) = -W^T H - Ksign(pD_t^{\alpha-1} e) + qD_t^{\alpha-1} e. \tag{19}$$

where $K = [k_1, k_2, \cdots, k_n]^T$ is the estimated value of the upper bound ρ_i^* of the optimal approximation error. In this paper, the adaptive law of the RBF neural network weight and the estimated value of the upper bound of the optimal approximation error were designed as follows:

$$\dot{W}_i = \lambda_i p(D_t^{\alpha-1} e_i(t)) H, \tag{20}$$

$$\dot{k}_i = \gamma_i (D_t^{\alpha-1} e_i(t)) p \cdot sign(pD_t^{\alpha-1} e_i(t)), \tag{21}$$

where $\lambda_1 and \gamma_i$ are the adjustment parameters of the adaptive law, and $\lambda_1 and \gamma_i$ are positive real numbers. p satisfies $p \cdot q < 0$. In the following subsection, stability analysis is given on the basis of the Lyapunov stability criterion.

3.3. Stability Analysis

The RBF neural network controller and its corresponding adaptive law are given in Section 3.2, and this subsection discusses whether the trajectory of the response system could reach the synchronization state with the driving system under this controller.

Proposition 2 Given the initial conditions, the adaptive RBF neural network controller proposed in this paper could realize the synchronization.

Proof. After the synchronization controller $U(t)$ proposed in the previous section had been introduced into the synchronization error system, the error system was organized as follows:

$$D_t^{\alpha} e_i(t) = \phi_i - W^T H - Ksign(pD_t^{\alpha-1} e) + qD_t^{\alpha-1} e. \tag{22}$$

It can be further deduced as follows:

$$D_t^{\alpha} e_i(t) = \rho_i - \widetilde{W}_i^T H - k_i sign(pD_t^{\alpha-1} e_i(t)) + qD_t^{\alpha-1} e_i(t). \tag{23}$$

The Lyapunov function was constructed as follows:

$$V = \frac{1}{2} \sum_{i=1}^{n} (D_t^{\alpha-1} e_i(t))^T \cdot pD_t^{\alpha-1} e_i(t) + \frac{1}{2} \sum_{i=1}^{n} \frac{1}{\lambda_i} \widetilde{W}_i^T \widetilde{W}_i + \frac{1}{2} \sum_{i=1}^{n} \frac{1}{\gamma_i} (k_i - \rho_i^*)^2, \tag{24}$$

where ρ_i^* is a positive real number. The fractional derivative of both sides of the following equation were taken:

$$\dot{V} = \frac{1}{2}\sum_{i=1}^{n}(D_t^{\alpha}e_i(t))^T \cdot p \cdot D_t^{\alpha-1}e_i(t) + \frac{1}{2}\sum_{i=1}^{n}(D_t^{\alpha-1}e_i(t))^T \cdot pD_t^{\alpha}e_i(t) + \sum_{i=1}^{n}\frac{1}{\lambda_i}\widetilde{W}_i^T\dot{\widetilde{W}}_i + \sum_{i=1}^{n}\frac{1}{\gamma_i}(k_i - \rho_i^*)\dot{k}_i. \tag{25}$$

By substituting adaptive laws λ_1, γ_i into the above equation, Equation (25) could be rearranged as follows:

$$\dot{V} \le \sum_{i=1}^{n}(D_t^{\alpha-1}e_i(t))^T \cdot (pq) \cdot D_t^{\alpha-1}e_i(t) + \sum_{i=1}^{n}(D_t^{\alpha-1}e_i(t))^T \cdot p\|\rho\| - \sum_{i=1}^{n}(D_t^{\alpha-1}e_i(t))^T \cdot p\|\rho^*\|. \tag{26}$$

In view of $0 \le |\rho_i| \le \rho^*$, the above equation can be reduced to

$$\dot{V} \le -\sum_{i=1}^{n} l \cdot (D_t^{\alpha-1}e_i(t))^2 \le 0, \tag{27}$$

where $l = -pq$. $0 \le V(t) \le V(0)$, that is, $V(t)$, is bounded. The integral of both sides of Equation (28) yield the following equation:

$$V(t) - V(0) \le l\int_0^t \sum_{i=1}^{n}(D_t^{\alpha-1}e_i(\tau))^2 \le l\int_0^t (D_t^{\alpha-1}e_i(\tau))^2. \tag{28}$$

This can be further deduced as follows:

$$\lim_{t\to+\infty}\int_0^t (D_t^{\alpha-1}e_i(\tau))^2 \le \frac{V(0) - \lim\limits_{t\to+\infty} V(t)}{l} \le \infty. \tag{29}$$

Then, $D_t^{\alpha-1}e_i(t) \in L_2$. The following formula can be derived from the synchronization error system:

$$\left\|D_t^{\alpha-1}e_i(t)\right\| \le \rho_i + \left\|\widetilde{W}_i^T\right\|\|H\| + |k_i| + |q||D_t^{\alpha}e_i(t)|. \tag{30}$$

Thus, $\|H\|$ is bounded. Then, $D_t^{\alpha}e_i(t) \in L_2 \cap L_\infty$ and $D_t^{\alpha}e_i(t) \in L_\infty$. It follows from Barbalat's lemma that $\lim\limits_{t\to+\infty} D_t^{\alpha}e_i(t) = 0$. Through Proposition 1, the following equation can be obtained:

$$\lim_{t\to+\infty} e_i(t) = 0. \qquad (i = 1, 2, \cdots, n) \tag{31}$$

So, the synchronization error asymptotically approached zero, and the proof of Proposition 2 is completed. □

4. Numerical Example

In order to verify the effectiveness of the controller presented in this paper, the improved predictor-corrector method [33] was applied to the numerical simulation of the fractional chaotic system. The controller in this paper is synchronous control in the case of the nonlinear function model of the chaotic system. The nonlinear uncertainty term and the external disturbance were completely unknown. The relevant models required for the simulation are given below.

4.1. Fractional-Order Time-Delay Chaotic System

The expression of the fractional delay Liu system [34] is as follows:

$$\begin{cases} D_t^{\alpha} x = a(y(t) - x(t-\tau)) \\ D_t^{\alpha} y = bx(t-\tau) - x(t)z(t), \\ D_t^{\alpha} z = cz(t-\tau) - dx^2(t) \end{cases} \tag{32}$$

when the order of the system iwass set as $\alpha = 0.97$, the control parameter $(a, b, c, d) = (10, 20, -2.5, 4)$, and the time delay $0 < \tau \leq 0.005$, the system was in a chaotic state. In this paper, time $\tau = 0.005$ was selected, the initial value state of the system iwass $(x_0, y_0, z_0) = (2.2, 2.4, 4.8)$, and the phase–space trajectory of the system is shown in Figure 1. The expression of the fractional delay financial system [35] is as follows:

$$\begin{cases} D_t^{\alpha} x_1 = z_1 - a_1 z_1 + x_1 y_1(t-\tau) \\ D_t^{\alpha} y_1 = 1 - b_1 y_1 + x^2(t-\tau) \\ D_t^{\alpha} z_1 = -x_1(t-\tau) - c_1 z_1 \end{cases}, \tag{33}$$

when the order of the system was $\alpha = 0.97$, control parameter $(a_1, b_1, c_1) = (3, 0.1, 1)$, and time delay $\tau = 0.001$, the system was in a chaotic state. In this paper, the initial value state of the system was $(x_0, y_0, z_0) = (0.1, 4, 0.5)$, and the phase–space trajectory of the system is shown in Figure 2.

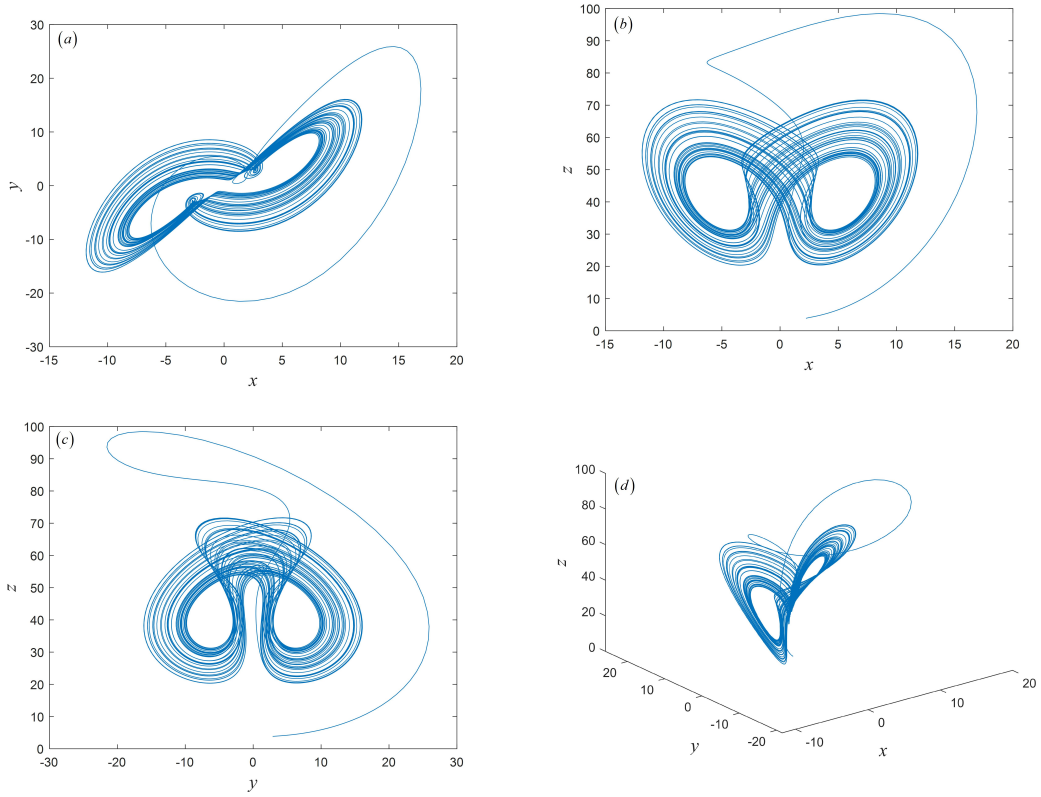

Figure 1. Phase–space trajectory distribution of fractional delay financial system: (**a**) X–Y plane; (**b**) X–Z plane; (**c**) Y–Z plane; (**d**) X–Y–Z plane.

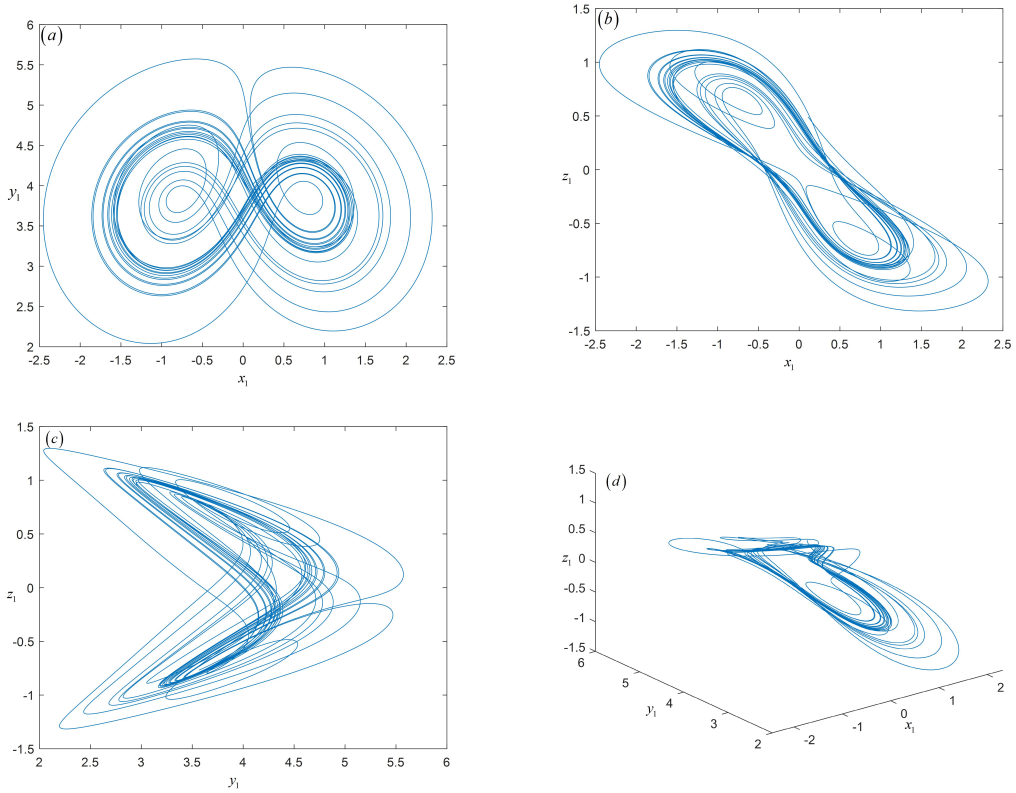

Figure 2. Phase–space trajectory distribution of fractional delay Liu system: (**a**) X–Y plane; (**b**) X–Z plane; (**c**) Y–Z plane; (**d**) X–Y–Z plane.

4.2. Simulation Results

In order to show the correctness and feasibility of the control method presented in this paper, the fractional delay Lu and financial system with uncertain terms and external disturbances were selected for numerical experiments. The expression of the driving system is as follows:

$$\begin{aligned} D_t^{\alpha} x &= f(x, x(t-\tau_2)) + \Delta f_1(x) + d_1(t) \\ &= \begin{bmatrix} a(x_2(t) - x_1(t-\tau_1)) \\ bx_1(t-\tau_1) - x_1(t)x_3(t) \\ cx_3(t-\tau_1) - dx_1^2(t) \end{bmatrix} + \begin{bmatrix} ecos(\pi t)x_1 \\ ecos(\pi t)x_2 \\ ecos(\pi t)x_3 \end{bmatrix} + \begin{bmatrix} fsin(t) \\ fsin(t) \\ fsin(t) \end{bmatrix}, \end{aligned} \tag{34}$$

and the expression of the response system is as follows:

$$\begin{aligned} D_t^{\alpha} y &= g(x, x(t-\tau_2)) + \Delta f_2(x) + d_2(t) + U(t) \\ &= \begin{bmatrix} y_3 - a_1 y_1 + y_1 y_2(t-\tau_2) \\ 1 - b_1 y_2 - y_1^2(t-\tau_2) \\ -y_1(t-\tau_2) - c_1 y_3(t) \end{bmatrix} + \begin{bmatrix} d_1 sin(\pi t) y_1 \\ d_1 sin(\pi t) y_2 \\ d_1 sin(\pi t) y_3 \end{bmatrix} + \begin{bmatrix} f_1 cos(t) \\ f_1 cos(t) \\ f_1 cos(t) \end{bmatrix} + \begin{bmatrix} u_1(t) \\ u_2(t) \\ u_3(t) \end{bmatrix}. \end{aligned} \tag{35}$$

From Equations (19), (34) and (35), the synchronization error system is as follows:

$$\begin{bmatrix} \rho_1 - \widetilde{W}_1^T H - k_1 sign(pD_t^{\alpha-1} e_1(t)) + qD_t^{\alpha-1} e_1(t) \\ \rho_2 - \widetilde{W}_2^T H - k_2 sign(pD_t^{\alpha-1} e_2(t)) + qD_t^{\alpha-1} e_2(t) \\ \rho_3 - \widetilde{W}_3^T H - k_3 sign(pD_t^{\alpha-1} e_3(t)) + qD_t^{\alpha-1} e_3(t) \end{bmatrix}. \tag{36}$$

From Proposition 2, driving system Equation (34) and response system Equation (35) could be synchronized under the action of the controller. The remaining unknown pa-

rameters selected in this paper were $e = 0.7$, $f = 1.3$, $e_1 = 0.2$, and $f_1 = 0.5$, and the input variables of the RBF neural network were synchronization error vectors e_1, e_2, e_3. The number of hidden layer neurons was 8, and the central matrix of the neurons was as follows:

$$C = \begin{bmatrix} -1.5 & 1 & -0.5 & 0 & 0.5 & 1 & 1.5 & 2 \\ -1.5 & 1 & -0.5 & 0 & 0.5 & 1 & 1.5 & 2 \\ -1.5 & 1 & -0.5 & 0 & 0.5 & 1 & 1.5 & 2 \end{bmatrix}. \tag{37}$$

The width value was $b_j = 3, (j = 1, 2, \cdots, 8)$, and the adaptive adjustment parameters were $\lambda_i = 3000, \gamma_i = 3.5, (i = 1, 2, 3)$. The initial weights of the neural network were 8 zero vectors, and the initial values of the adaptive law were $k_i(0) = 0.4, (i = 1, 2, 3)$. The values of p and q were $p = 0.9, q = -10$. The time step was $h = 0.001$ for the numerical simulation. Figure 3a shows that the synchronization error converged quickly, indicating that the designed RBF neural network had a good approximation effect. Figure 3b–d show that each state synchronized well. Figure 4 shows that the amplitude of the weight of the RBF neural network was not large, and the change was relatively stable, which indicates that the control effect of the synchronous controller presented in this paper was better.

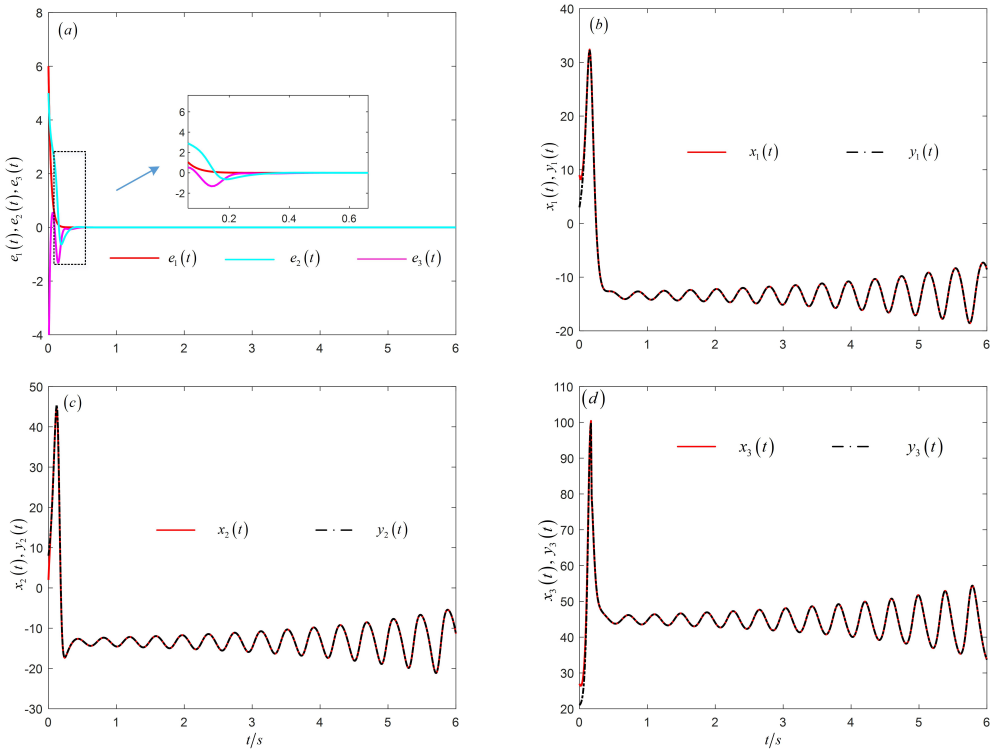

Figure 3. State trajectories of synchronization error vectors (**a**) e_1, e_2,and e_3, (**b**) x_1 and y_1, (**c**) x_2 and y_2, and (**d**) x_3 and y_3.

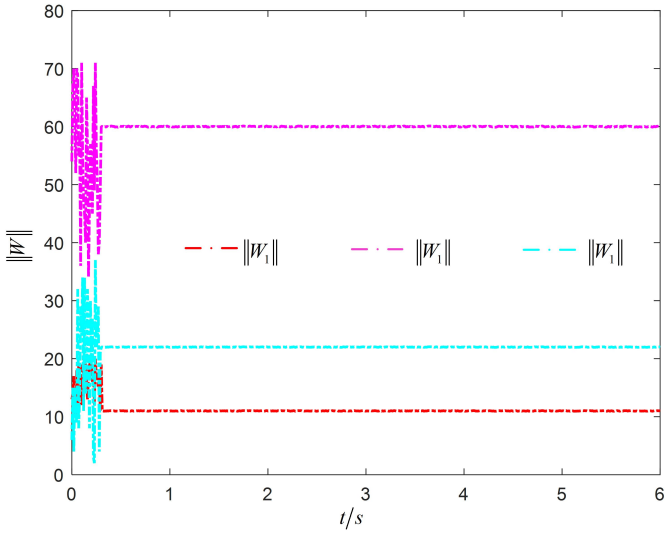

Figure 4. The optimal weight value of the neural network.

5. Conclusions

An adaptive RBF neural network controller and an integer-order parameter adaptive law were presented for the synchronization of a heterogeneous structured fractional-order chaotic system with completely unknown nonlinear uncertainties and external disturbances. The controller and the RBF neural network were combined with adaptive control technology. On the one hand, the unknown nonlinear function was approximated with an RBF neural network. On the other hand, an adaptive law was used to adjust the corresponding parameters in the controller. Numerical simulation results show that the controller designed in this paper not only realized the synchronization control of heterogeneous structure fraction-order time-delay chaotic systems, but also had fast response speed, a good control effect, and strong anti-interference ability. In future work, we will construct a secure communication scheme on the basis of this synchronization scheme that forms an encrypted signal by driving the sequence generated by the system and the signal to be encrypted, the decryptor decrypts the encrypted signal in response to the sequence generated by the system, and the recovered signal is obtained. Therefore, the results of this study are not only of great theoretical importance, but also have great application value in the field of secure communication.

Author Contributions: Conceptualization, W.Y. and Q.D.; methodology, W.Y.; software, W.Y.; validation, Z.J., X.H. and W.Y.; formal analysis, W.Y.; project administration, Q.D.; funding acquisition, Q.D. and W.Y. All authors have read and agreed to the published version of the manuscript.

Funding: This research were funded by the National Natural Science Foundation of China (61471158) and the Graduate Innovative Science Research Project of Heilongjiang University in 2022 (NYJSCX2022-023HLJU).

Institutional Review Board Statement: Not applicable.

Informed Consent Statement: Not applicable.

Data Availability Statement: Data sharing is not applicable to this article, as no datasets were generated or analyzed during the current study.

Conflicts of Interest: The authors declare no conflict of interest.

References

1. Rakkiyappan, R.; Chandrasekar, A.; Lakshmanan, S. Effects of leakage time-varying delays in Markovian jump neural networks with impulse control. *Neurocomputing* **2013**, *121*, 365–378. [CrossRef]
2. Rakkiyappan, R.; Chandrasekar, A.; Lakshmanan, S. Exponential stability of Markovian jumping stochastic Cohen-Grossberg neural networks with mode-dependent probabilistic time-varying delays and impulses. *Neurocomputing* **2014**, *131*, 265–277. [CrossRef]
3. Li, T.; Wang, T.; Song, A.; Fei, S. Combined convex technique on delay-dependent stability for delayed neural networks. *IEEE Trans. Neural Netw. Learn. Syst.* **2013**, *24*, 1459–1466. [CrossRef] [PubMed]
4. Deng, Y.M.; Fan, H.F.; Wu, S.M. A hybrid ARIMA-LSTM model optimized by BP in the forecast of outpatient visits. *J. Ambient Intell. Humaniz. Comput.* **2020**. [CrossRef]
5. Deng, W.; Li, C.; Lu, J. Stability analysis of linear fractional differential system with multiple time delays. *Nonlinear Dyn.* **2007**, *48*, 409–416. [CrossRef]
6. Xiao, M.; Zheng, W.; Cao, J. Bifurcation and control in a neural network with small and large delays. *Neural Netw.* **2013**, *44*, 132–142. [CrossRef]
7. Choi, S.W.; Kim, B.H.S. Applying PCA to Deep Learning Forecasting Models for Predicting PM2.5. *Sustainability* **2021**, *13*, 3726. [CrossRef]
8. Xiao, D.Y.; Su, J.X. Research on Stock Price Time Series Prediction Based on Deep Learning and Autoregressive Integrated Moving Average. *Sci. Program.-Neth.* **2022**, *2022*, 4758698. [CrossRef]
9. Aghababa, M. Control of fractional-order systems using chatter-free sliding mode approach. *J. Comput. Nonlinear Dyn.* **2014**, *9*, 031003. [CrossRef]
10. Aghababa, M. No-chatter variable structure control for fractional nonlinear complex systems. *Nonlinear Dyn.* **2013**, *73*, 2329–2342. [CrossRef]
11. Aghababa, M. Synchronization and stabilization of fractional second-order nonlinear complex systems. *Nonlinear Dyn.* **2015**, *80*, 1731–1744. [CrossRef]
12. Pecora, L.; Carroll T. Synchronization in chaotic system. *Phys. Rev. Lett.* **1990**, *64*, 821–824. [CrossRef] [PubMed]
13. Megherbi, O.; Hamiche, H.; Djennoune, S. A New Contribution for the Impulsive Synchronization of Fractional-Order Discrete-Time Chaotic Systems. *Nonlinear Dyn.* **2017**, *980*, 1519–1533. [CrossRef]
14. Park, J.H. Adaptive modified projective synchronization of a unified chaotic system with an uncertain parameter. *Chaos Solitons Fractals* **2017**, *34*, 1552–1559. [CrossRef]
15. Mobayen, S. Chaos Synchronization of Uncertain Chaotic Systems Using Composite Nonlinear Feedback Based Integral Sliding Mode Control. *ISA Trans.* **2018**, *77*, 100–111. [CrossRef] [PubMed]
16. Sangyun, L.; Mignon, P.; Jaeho, B. Robust adaptive synchronization of a class of chaotic systems via fuzzy bilinear observer using projection operator. *Inf. Sci.* **2017**, *402*, 182–198.
17. Chou, H.; Chuang, C.; Wang, W. A Fuzzy-Model-Based Chaotic Synchronization and Its Implementation on a Secure Communication System. *IEEE Trans. Inf. Forensics Secur.* **2013**, *8*, 2177–2185. [CrossRef]
18. Xu, G.; Xu, J.; Xiu, C.; Liu, F.; Zang, Y. Secure communication based on the synchronous control of hysteretic chaotic neuron. *Neurocomputing* **2017**, *227*, 108–112. [CrossRef]
19. Mainieri, R.; Rehacek, J. Projective synchronization in three-dimensional chaotic systems. *Phys. Rev. Lett.* **1999**, *82*, 3024–3045. [CrossRef]
20. Velmurugan, G.; Rakkiyappan, R. Hybrid Projective Synchronization of Fractional-Order Chaotic Complex Nonlinear Systems with Time Delays. *J. Comput. Nonlinear Dyn.* **2016**, *11*, 031016. [CrossRef]
21. Wang, S.; Yu, Y.; Wen, G. Hybrid projective synchronization of time-delayed fractional order chaotic systems. *Nonlinear-Anal.-Hybrid Syst.* **2014**, *11*, 129–138. [CrossRef]
22. Wang, X.Y.; He, Y.J. Projective synchronization of fractional order chaotic system based on linear separation. *Phys. Lett. A* **2008**, *372*, 435–441. [CrossRef]
23. Bao, H.B.; Cao, J. Projective synchronization of fractional-order memristor-based neural networks. *Neural Netw.* **2015**, *63*, 1–9. [CrossRef]
24. Zhou, P.; Zhu, W. Function projective synchronization for fractional-order chaotic systems. *Nonlinear Anal. Real World Appl.* **2011**, *12*, 811–816. [CrossRef]
25. Chen, J.; Zeng, Z.; Jiang, P. Global Mittag–Leffler stability and synchronization of memristor-based fractional-order neural networks. *Neural Netw.* **2014**, *51*, 1–8. [CrossRef]
26. Wang, X.Y.; Zhang, X.P.; Ma, C. Modified projective synchronization of fractional-order chaotic systems via active sliding mode control. *Nonlinear Dyn.* **2012**, *69*, 511–517. [CrossRef]
27. Yu, J.; Hu, C.; Jiang, H.; Fan, X. Projective synchronization for fractional neural networks. *Neural Netw.* **2014**, *49*, 87–95. [CrossRef]
28. Wang, S.; Yu, Y.G.; Diao, M. Hybrid projective synchronization of chaotic fractional order systems with different dimensions. *Phys. A* **2010**, *389*, 4981–4988. [CrossRef]
29. Wu, R.C.; Hei, X.D.; Chen, L.P. Finite-time stability of fractional-order neural networks with delay. *Commun. Theor. Phys.* **2013**, *60*, 189–193. [CrossRef]

30. Lazarevic, M.; Debeljkovic, D. Finite time stability analysis of linear autonomous fractional order systems with delayed state. *Asian J. Control* **2005**, *7*, 440–447. [CrossRef]
31. Lazarevic, M.; Spasic, A. Finite-time stability analysis of fractional order time-delay systems: Gronwall's approach. *Math. Comput. Model.* **2009**, *49*, 475–481. [CrossRef]
32. Lorenz, C.; Hartley, T. Variable order and distributed order fractional operators. *Nonlinear Dyn.* **2002**, *29*, 57–98. [CrossRef]
33. Samko, S.; Kilbas, A.; Marichev, O. *Fractional Integrals and Derivatives*; Gordon and Breach Science Publishers: Basel , Switzerland, 1993.
34. Gorenflo R.; Mainardi F. *Fractional Calculus*; Springer: New York, NY, USA, 1997.
35. Liu, H.; Pan, Y.; Li, S. Adaptive fuzzy backstepping control of fractional-order nonlinear systems. *IEEE Trans. Syst. Man Cybern. Syst.* **2017**, *47*, 2209–2217. [CrossRef]